Coaxial microwave resonant sensor design for monitoring ionic concentration in aqueous solutions

Subhanwit Roy
Department of Electrical and Computer Engineering
Iowa State University
Ames IA, United States
roys@iastate.edu

Nathan M. Neihart
Department of Electrical and Computer Engineering
Iowa State University
Ames IA, United States
neihart@iastate.edu

Nicola Bowler
Department of Materials Science and Engineering
Department of Electrical and Computer Engineering
Center for Nondestructive Evaluation
Iowa State University
Ames IA, United States
nbowler@iastate.edu

***Abstract*—Nitrate efflux from agricultural lands mixes with surface streams and adversely affects both human health as well as aquatic life. Currently, there is a lack of low-cost, effective, real-time systems for monitoring ion concentration. In this work, a microwave resonant sensor is designed using an open-ended coaxial transmission line, which can be evanescently perturbed by a liquid sample, and a suitable coupling structure which allows transmission measurements. The sensor is developed to have high sensitivity at agriculturally relevant concentrations, low manufacturing costs, and small dimensions to be potentially field deployable. Finite Element Analysis simulations are carried out using ANSYS HFSS, employing complex permittivity data of aqueous solution samples with varying concentrations of nitrate, sulfate, and chloride ions. Appropriate functions are determined that model the correlations between resonant frequency and ion concentration, and discussion on the feasibility of the sensor for field deployment is presented.**

Keywords—dielectric metrology, low cost, microwave resonant sensor, nitrate monitoring, nondestructive, noninvasive

I. INTRODUCTION

In the agricultural croplands of the Midwestern United States, subsurface tile drainage is predominantly used to remove excess moisture from the soil. However, owing to the fact that tile drainage provides for a flow-path to the surface streams, excess nutrients from the croplands are washed directly to these streams. This creates an imbalance of the ions present in bodies of surface water, and in turn affects both aquatic as well as human life. Of all the excess ions found in tile drainage water [1], nitrate ion (NO_3^-) has the most significant impact. Nitrates, which enter the soil through fertilizers, are washed into the river systems and lead to explosive algae growth, which, in turn, depletes the oxygen content of water. This phenomenon is called hypoxia and it is deleterious to aquatic life. Nitrates in drinking water adversely affect human health, most notably causing blue baby syndrome. In addition, nitrates increase the risk of bladder, colon, and rectum cancers, and cause birth defects, besides posing other threats.

The lack of effective nitrate management strategies drives high costs of nitrate treatment of water. In Des Moines, Iowa, the cost of nitrate treatment of drinking water is about $7,000 per day [2]. A major reason behind this high cost is the lack of an affordable, effective ion monitoring system. The need to operate with low, agriculturally relevant concentrations renders many of the classical methods of measuring ionic concentration ineffective for the problem herein. The fact that the ionic concentration of drainage water is tightly associated with local hydrology and rapidly changes with space and time implies that laboratory methods based on spot and snapshot sampling are not useful, thus calling for the need of a real time system. Currently, there are two predominant approaches in literature for real-time ion monitoring, viz. the Ion Selective Electrode (ISE) sensor [3], and the Ultraviolet (UV) Absorption sensor [4]. The former is an electrochemistry based technique which is inexpensive (~$600) and has a fast response time. However, it is seldom selective to only one ion, which causes interference in concentration measurement, and has low durability. The latter, which operates on the ability of a sample to absorb ultraviolet radiation, also has a rapid response time, but is very expensive ($16,000-$25,000) and requires a highly monochromatic source of UV radiation, besides being prone to interference by other ions and organic compounds.

Hence, there is a need to develop a new technique for real-time ion sensing of tile-drainage water. This paper discusses an approach based on dielectric metrology to design a highly sensitive ion monitoring microwave resonant sensor which is potentially low cost, nondestructive, and field deployable. The method undertaken in this research is novel because, to our knowledge, no other group has used a resonant method to characterize ionic solutions.

Section II discusses the dielectric characterization of ionic samples which drives the choice of the method adopted for sensor design. Section III explores the design of an evanescently perturbed coaxial resonant sensor and its modeling by HFSS. The simulation results are analyzed in Section IV, and Section V concludes the paper with a discussion on the feasibility of the sensor for field deployment.

This work is funded by USDA-National Institute of Food & Agriculture, Award Number 013025-00001.

II. Method

A. Dielectric Spectroscopy

Dielectric spectroscopy involves measuring the complex relative permittivity ε_r of a sample over a frequency spectrum [5], which can be expressed as

$$\varepsilon_r(f) = \varepsilon_r'(f) - j\varepsilon_r''(f) \quad (1)$$

The real part of permittivity of indicates the ability of the medium to become polarized by an external electric field, whereas the imaginary part quantifies losses due to absorption of electrical energy upon the application of the external field. For an electrolyte solution, these two components of the complex relative permittivity can be attributed to three additive contributions, viz. intramolecular forces, intermolecular forces, and migration of charge carriers under an applied electric field (conductivity). The conductivity term contributes solely to the dissipation of energy leading to a more informative version of (1).

$$\varepsilon_r(f) = \varepsilon_r'(f) - j\left[\varepsilon_d''(f) + \frac{\sigma}{2\pi\varepsilon_0 f}\right] \quad (2)$$

In (2), ε_r'' has been decomposed using a dipolar loss component ε_d'' and a dc conductivity term σ. Fig. 1 demonstrates the shape of the dielectric spectrum of deionized water at a fixed temperature. A relaxation mechanism can be observed around 20 GHz, which corresponds to the relaxation of hydrogen bonded water molecules. Such a spectrum can be represented by a single-term Debye term relaxation model which uses the fitting parameter ε_{dc} (static real permittivity), τ (relaxation time) and ε_∞ (high frequency real permittivity) [6]. Further, σ (dc conductivity) is required to represent the conductive loss in the imaginary permittivity. Upon addition of ions, hydration layers are formed by water molecules surrounding the ions, and these give rise to another relaxation process around in the microwave region with a relaxation frequency f_{relax} ~ 20 GHz [6]. As ionic concentration of an aqueous solution increases, the shape of the dielectric spectrum changes, leading to change in the values of the fitting parameters. Hence, in theory, the change in dielectric properties of a sample can be used to infer its ionic concentration. It should be noted that other non-rotational relaxation processes which take place in the infrared and ultraviolet frequencies have not been considered herein.

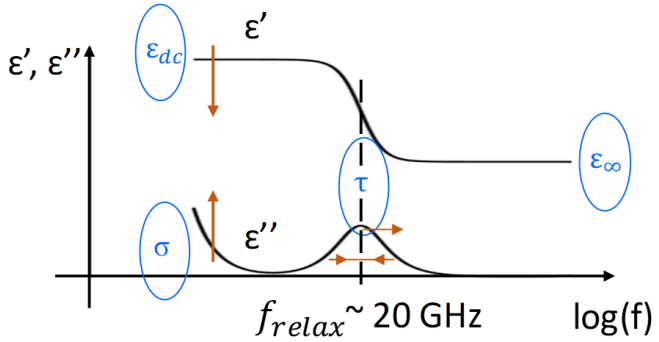

Fig. 1 Shape of dielectric spectrum of water at a fixed temperature, arrows show shifts in the dielectric spectrum for large changes in ionic concentration

TABLE I. Concentration of different samples tested

Electrolyte Solution	Concentrations Tested (mmol/L)
Sodium Nitrate	0 to 28.56
Sodium Sulfate	0 to 12.48
Sodium Chloride	0 to 11.28

B. Sample Characterization

A Speag open-ended coaxial DAK3.5 dielectric probe kit (recommended bandwidth of 200 MHz to 20 GHz) was used in conjunction with an Anritsu 37347C Vector Network Analyzer (VNA), with a nominal bandwidth of 40 MHz to 20 GHz, to investigate the dielectric spectra of fifteen different concentrations of three different salt solutions, as listed in Table I, along with deionized water. The temperature of the samples was maintained at 25 ºC ± 0.01 ºC. A separate Seven2Go™ conductivity meter was used with an InLab720 probe was used to measure the dc conductivity. The measurements were carried out across a broadband frequency range 200 MHz to 20 GHz. The dielectric characterization experiment has been described in detail in [6].

C. Dielectric Measurement Techniques

Continued interest in the molecular structure of polar dielectric liquids, and the use of polar liquids as dielectric reference materials and to manufacture tissue-equivalent materials have led to significant research in dielectric metrology. The fact that dipolar relaxations generally occur in the microwave region of the spectrum for polar liquids helps narrow down the frequency range of interest.

One of the most commonly used and studied families of microwave dielectric techniques is broadband dielectric spectroscopy. This method involves applying a time-varying electric field to a sample under test and measuring either the power reflected by the sample (reflectometric methods) or the power transmitted through it (transmission methods) with the use of a VNA. Such methods provide dielectric information about a broad range of frequencies. Interfacing the sample with the sensor is more convenient with reflectometric methods, making the open ended coaxial probe the most widely used broadband technique [7].

Resonant methods form the other prevalent class of dielectric techniques. These methods employ resonators to infer the complex permittivity of samples from the measurement of resonant frequency and Q-factor. Such techniques provide dielectric information only at discrete resonant frequencies. Various kinds of resonant dielectric sensors are found in literature, of which the most common are cavity resonators, followed by dielectric resonators. Open ended coaxial transmission line resonators, operating in transverse electromagnetic (TEM) mode, have also been demonstrated in literature [8].

D. Choice of Dielectric Measurement Method

The goal of this research is to develop a low cost, high sensitivity, nondestructive, real-time sensor which is field deployable. The need for an expensive VNA to make broadband measurements limits their usability outside the laboratory. On the other hand, resonant methods are not able to provide a complete picture of the dielectric spectrum, in spite of requiring cheaper instrumentation and having higher sensitivity [9]. Since this work aims to develop an affordable, field deployable sensor which can measure changes in ionic concentration, a comprehensive picture of the entire dielectric spectrum is not required. Hence, a resonant method is chosen.

Cavity resonators cannot be perturbed noninvasively by a sample, requiring additional design. Dielectric resonators, which allow noninvasive perturbation, often require disk-shaped samples, making them difficult to be perturbed by liquid samples and call for design of microfluidic structures. Hence, a simple open-ended coaxial transmission line resonator is chosen, which can be perturbed evanescently by the sample at the open end.

III. Resonant Sensor Design

A. Transmission Line Resonator Theory

A section of a transmission line resonates when its boundary conditions allow an incident wave to be reflected repeatedly from its ends to form a standing wave. For an open-ended piece of transmission line, this condition amounts to its length being an integer multiple of the half-wavelength of the incident wave, and the corresponding frequency is then called the resonant frequency. For an open-ended piece of coaxial transmission line, the resonant frequencies f_n are given by

$$f_n = \frac{(n+1)c}{2L\sqrt{\varepsilon_m'}} \tag{3}$$

In (3), c denotes the phase velocity of the electromagnetic wave in free space (approximately 3×10^8 m/s), L stands for the length of the coaxial line, ε_m' represents the permittivity of its dielectric layer and n denotes the resonant mode (n=0 being the fundamental mode. It can be observed that for a given type of coaxial transmission line, its fundamental resonant frequency f_0 is inversely related to its axial length L.

B. Resonator Perturbation Theory

Perturbation theory describes the effect of introducing a perturbation in the form of an external material or a change in shape of a resonator on its resonant characteristics, and was initially developed by Waldron [10] for a cavity. It showed that such perturbations led to a shift in the resonant frequency and a change in Q-factor. The derived formula holds true only for cavities, but the theory has been used for analysis of open ended coaxial resonators [11]. Thus, for the problem herein, even though an exact prediction of the relationship cannot be made at this stage, a change in resonant frequency can be expected to be observed with change in ionic concentration.

C. Choice of Resonator Dimensions

The need for a low-cost resonator with high durability and low loss suggests the choice of a 50 Ω standard RG401 coaxial cable for the resonator design. RG401 has an inner conductor diameter of 1.63 mm, dielectric spacer diameter of 5.31 mm, and outer shield diameter of 6.35 mm. It uses a polytetrafluoro-ethylene (PTFE) spacer with $\varepsilon_m' \approx 2.1$.

A study conducted in [12] reveals that in the frequency range of 200 MHz to 20 GHz, the lower the frequency, the higher is the sensitivity of the complex permittivity of an aqueous solution to changes in ionic concentration. For a fixed type of coaxial line, (3) calls for the use of a longer axial length to get a lower resonant frequency and, in turn, higher sensitivity. The requirement for the sensor to be field deployable, however, puts a limit on its maximum length. Thus, a trade-off is made and an length L = 10.35 cm is chosen as the final dimension, to enable the resonator to fit inside a standard 12.7 cm diameter tile drainage pipe. This length corresponds to an ideal open-ended resonant frequency of 1 GHz when the resonator is interfaced with free space.

D. Coupling Structure Design

To excite the resonant modes and measure the resonance characteristics of a resonant sensor, it is necessary to couple some energy in and out of the resonator. This can be done either noninvasively at the end of the coaxial resonator which is not interfaced with the sample, or invasively at any point on the resonator, which would require additional design. It is important to not couple too much energy from the resonator, as it would severely load the resonator, drastically affecting its resonant characteristics. Hence, to measure the resonance reliably, and to save on extra design costs, a noninvasive weak coupling technique is desired.

Resonator fields can be coupled to another device either capacitively or inductively. The former can be done using an RF connector with a straight, protruding inner conductor to match the electric fields of the resonator and the connector, while the latter can be achieved by matching magnetic fields using an RF connector with a looped inner conductor. Inductive coupling loops tend to resonate themselves [13], thus interfering with the resonant characteristics of the resonator, making them unsuitable for the current purpose.

A capacitive coupling structure can be designed to either measure the reflection coefficient looking into the resonator, or to take transmission measurements between two ports. Measuring a weakly coupled resonance using a reflection method is challenging because the weak coupling leads to a reflection coefficient very close to 0 dB, and such an attempt is considered to be a “bad practice” by a National Physical Laboratory, UK report [14].

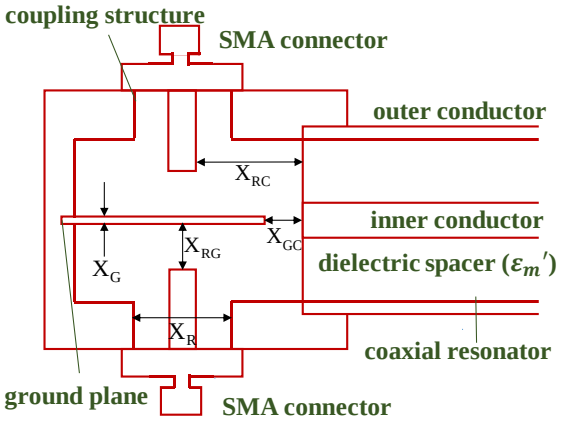

Fig. 2 Schematic cross-section of coupling structure with coaxial resonator

Rowe et al [8] developed a noninvasive, capacitive coupling structure, which enabled single ended transmission coupling, which keeps the other end of a coaxial resonator available for evanescent perturbation by a liquid sample. The cross sectional view of this coupling structure is shown in Fig 2. It consists of two symmetric coupling mounts with a thin ground plane in between, which prevents crosstalk between two SMA connectors placed symmetrically on either coupling mount. The SMA connectors can be connected to an appropriate measuring instrument to measure transmission parameters. The coupling strength is dominated by the dimensions X_{RC} : distance between SMA receptacle and resonator, X_{GC} : distance between ground plane and resonator, X_{RG} : distance between SMA receptacle and ground plane, X_G : thickness of ground plane, and X_R : radius of hole housing the SMA receptacle. X_R is set such that the hole forms a 50 Ω transmission line to facilitate impedance match with a standard 50 Ω SMA connector.

The coupling structure with the optimum dimensions given in [8], along with the coaxial resonator were modeled on ANSYS HFSS. The SMA connector was modeled following the dimensions of a standard 50 Ω SMA connector (Digi-Key 1052422-1) and this set $X_R = 3\text{mm}$. In the model, a wave port was placed on each SMA connector, and the entire system was placed inside a radiation box made partly of air, and the rest of the varying sample to replicate a practical situation, to impose a radiation boundary condition. The model was drawn to simulate the resonator being dipped to a length of 3.35 cm inside the solution under test.

The sensor was simulated for air and deionized (DI) water samples using broadband adaptive meshing and a frequency

TABLE II. FINAL OPTIMIZED COUPLING STRUCTURE DIMENSIONS WHICH DOMINATE COUPLING STRENGTH

X_{RC}	X_{GC}	X_{RG}	X_G
0.96 mm	0.25 mm	0.50 mm	0.50 mm

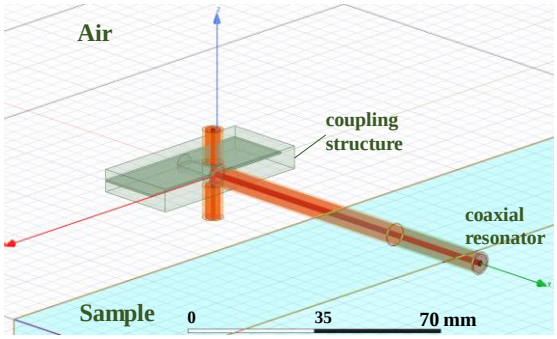

Fig. 3 Resonant sensor model on HFSS

range of 300 MHz to 3.3 GHz with a step size of 250 kHz. The simulations resulted in a fundamental resonant frequency of 980.6 MHz and 770.4 MHz for air and DI water respectively, along with two other higher modes of resonance in each case. It can be observed that the fundamental resonant frequency of the resonant sensor for air is close to 1 GHz, which is the ideal unloaded resonant frequency of the open ended coaxial line. The magnitude of the transmission scattering parameter S_{21} at resonance was, however, very low (-93.6 dB and -105.6 dB respectively), and this called for further optimization of the coupling structure dimensions. For this purpose, a series of simulations were run by varying X_{RC}, X_{GC}, and X_{RG}, respectively [12]. The final chosen dimensions which dominated coupling strength are presented in Table II. With these dimensions, for DI water sample, a fundamental resonant frequency of 765.8 MHz was observed, with an increase in $|S_{21}|$ at resonance by over 50 dB. Fig. 3 shows the model of the resonant sensor as designed on HFSS.

IV. RESULTS AND DISCUSSION

A. Simulation Results

The resonant sensor is simulated on HFSS for all the different sample types and concentrations discussed in Section IIB. The sample data is input to the simulator in terms of the real permittivity and loss tangent of the blue box in Fig. 3, which represents the sample solution. Figure 4 shows the $|S_{21}|$ response in dB for deionized water (c =0) and two different concentrations of sodium nitrate solution. It can be observed from Fig. 4 that as the concentration of nitrate ions increases, the resonant frequency of the sensor decreases for the three modes of resonance. Similar results are obtained for sulfate and chloride ions [12].

B. Curve Fitting and Discussion

For the three modes of resonance studied, the negative of the shift in resonant frequency from deionized water is plotted against ionic concentration for each of the three types of sample under test. For all three ions, Modes 1 and 2 show similar behavior and are fitted with an exponential model using nonlinear least-squares.

$$-\Delta f_r = \gamma_{r,1}(1-e^{-\gamma_{r,2}c}) \text{ for } r \in \{1,2\} \quad (4)$$

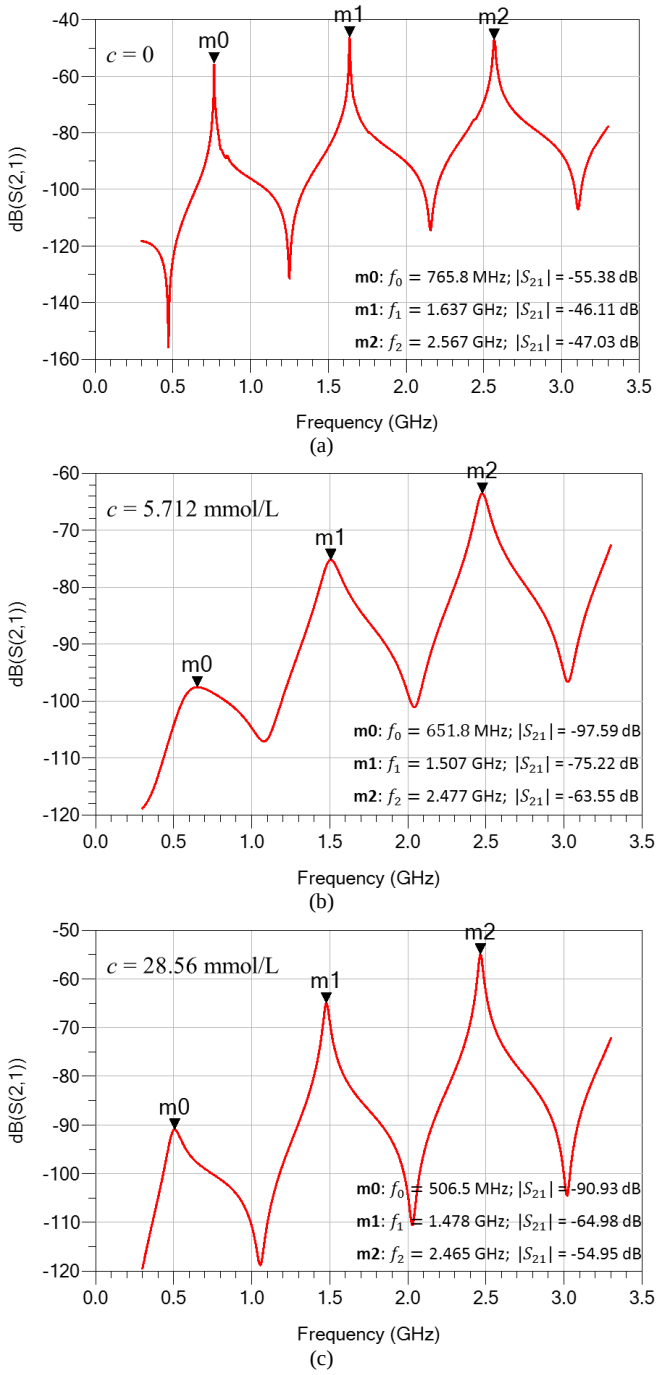

Fig. 4 Response of resonant sensor for sodium nitrate solution samples with concentration (a) c = 0, (b) c = 5.712 mmol/L, and (c) c = 28.56 mmol/L

In (4), r is the mode number, and $\gamma_{r,1}$ and $\gamma_{r,2}$ are fitting parameters. Trying to fit the mode 0 data with the same model yields good agreement for the higher concentrations, but overestimates the shift in resonant frequency for the lower ionic concentrations. For this purpose, an additional term with three fitting parameters is used to produce a good fit for the mode 0 data, as shown in (5), where $\gamma_{0,1}$, $\gamma_{0,2}$, $\gamma_{0,3}$, $\gamma_{0,4}$ and $\gamma_{0,5}$ are the fitting parameters.

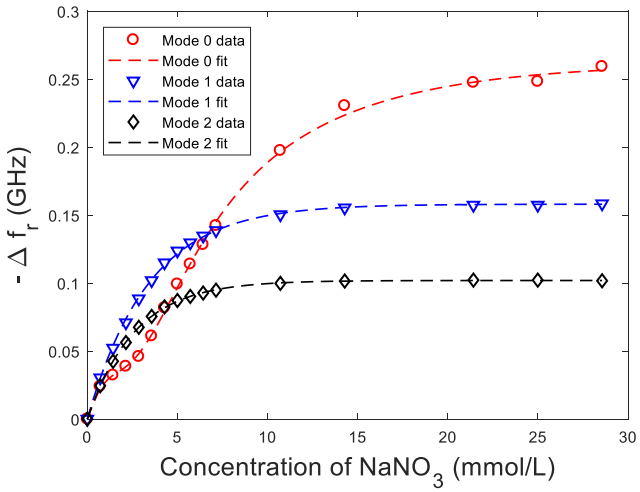

Fig. 5 Negative of the shift in resonant frequency from deionized water plotted against ionic concentration of sodium nitrate sample for the first three modes of resonance along with fitted models (dashed lines)

$$-\Delta f_0 = \gamma_{0,1}(1-e^{-\gamma_{0,2}c}) - (\gamma_{0,3}ce^{-c^{\gamma_{0,4}}})^{\gamma_{0,5}} \quad (5)$$

The resonant frequency data, along with the corresponding fitted curves are presented in Fig. 5. Similar results are obtained for sulfate and chloride ions. The fitting parameters used for curve fitting of Mode 0 using (5) is presented in Table III whereas Table IV lists the fitting parameters for curve fitting of Modes 1 and 2 using (4). The corresponding mean squared error (MSE) values of the fits are also reported. It can be observed that all MSE values are in the order of 10^{-4} or better, indicating the high quality of the fits.

A 10 mg/L standard is set for the maximum contaminant level (MCL) of nitrate-nitrogen in drinking water, which corresponds to 0.7139 mmol/L concentration of nitrate ions. On addition of this concentration to DI water, the shifts in resonant frequency for the first three resonant modes of the designed sensor are 22.02 MHz, 29.82 MHz, and 24.20 MHz respectively. It can be observed that for the fundamental mode, the shift in resonant frequency, is ~3% of the reference DI

TABLE III. VALUES OF FITTING PARAMETERS USED AND CORRESPONDING MEAN SQUARED ERRORS OF FITTING (MSE) FOR MODE 0 FOR SODIUM NITRATE, SODIUM SULFATE, AND SODIUM CHLORIDE SOLUTIONS

Sample Type	$\gamma_{0,1}$ [GHz]	$\gamma_{0,2}$ [L/mmol]	$\gamma_{0,3}$	$\gamma_{0,4}$	$\gamma_{0,5}$	MSE
Sodium Nitrate	0.262	0.137	1.07	0.518	5.46	1.08×10^{-5}
Sodium Sulfate	0.265	0.256	1.25	0.701	4.99	2.39×10^{-6}
Sodium Chloride	0.349	0.0774	1.64	0.536	16.5	1.04×10^{-4}

TABLE IV. VALUES OF FITTING PARAMETERS USED AND CORRESPONDING MEAN SQUARED ERRORS OF FITTING (MSE) FOR MODES 1 AND 2 FOR SODIUM NITRATE, SODIUM SULFATE, AND SODIUM CHLORIDE SOLUTIONS

Sample Type	Mode (r)	$\gamma_{r,1}$ [GHz]	$\gamma_{r,2}$ [L/mmol]	MSE
Sodium Nitrate	1	0.158	0.293	1.80×10^{-6}
	2	0.102	0.380	1.16×10^{-7}
Sodium Sulfate	1	0.158	0.620	1.56×10^{-6}
	2	0.106	0.748	1.71×10^{-4}
Sodium Chloride	1	0.160	0.278	1.65×10^{-5}
	2	0.102	0.370	9.72×10^{-6}

water frequency, and can be separated using a suitable frequency counting technique.

The sensitivity of the resonant sensor for a given mode of resonance is defined by $|\partial f_r / \partial c|$. It has been observed that the sensitivity varies with concentration for the three modes of resonance, for each ion type. The sensitivity of the sensor is high at lower concentrations, which are environmentally relevant, as shown by Fig. 6, which is obtained by plotting the derivatives of the fitted functions, for the three resonant modes.

V. CONCLUSION

The coaxial resonant sensor developed herein has been designed for measuring changes in ionic concentration of aqueous solution in the order of mmol/L. The sensor does not need an expensive VNA, unlike broadband methods, as it measures a shift in resonant frequency. It is designed to be constructed from inexpensive, readily-available RG401 coaxial cable, and a copper coupling structure, making it potentially low-cost. Thus, the developed sensor potentially bridges the gap in available literature between reliable ionic concentration monitoring at agriculturally relevant levels and economic feasibility.

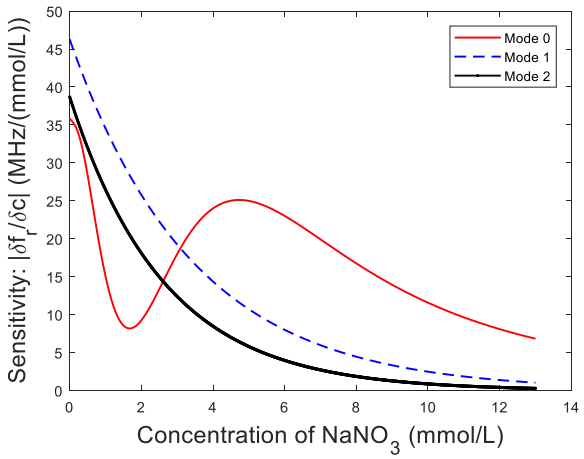

Fig. 6 Sensor sensitivity to the change in concentration of nitrate ions for the first three resonant modes

The next important step in the work is to test the sensor design under laboratory conditions with various types and concentrations of ionic solutions. This could be followed by using a comparatively low cost frequency measurement system to measure the frequency shift and dispense with the expensive VNA. The sensitivity of the sensor to manufacturing and measurement uncertainties needs to be analyzed. There also needs to be an investigation of the dielectric properties of multi-ionic systems to throw light onto how to modify the coaxial resonant sensor to detect ions in a practical situation, which is likely to involve water with multiple ionic and non-ionic species.

REFERENCES

[1] B. A. Zimmerman, "Exploration of ion species in agricultural subsurface drainage waters," M.S., Iowa State University, United States -- Iowa, 2016.

[2] "Nitrate levels hit record highs in 2 D.M. rivers," *Des Moines Register*. https://www.desmoinesregister.com/story/money/agriculture/2014/12/04/high-nitrates-des-moines/19906717/. [Accessed: 02-Dec-2017].

[3] E. M. Gross, R. S. Kelly, and D. M. Cannon, "Analytical Electrochemistry: Potentiometry," 2008.

[4] B. A. Pellerin, B. A. Bergamaschi, B. D. Downing, J. F. Saraceno, J. D. Garrett, and L. D. Olsen, "Optical techniques for the determination of nitrate in environmental waters: Guidelines for instrument selection, operation, deployment, maintenance, quality assurance, and data reporting," U.S. Geological Survey, Reston, VA, USGS Numbered Series 1-D5, 2013.

[5] A. Volkov and A. Prokhorov, "Broadband Dielectric Spectroscopy of Solids," *Radiophys. Quantum Electron.*, vol. 46, no. 8/9, pp. 657–665, Aug. 2003.

[6] A. Gorji, A. Kaleita, and N. Bowler, "Towards low-cost sensors for real-time monitoring of contaminant ions in water sources," in *2017 IEEE MTT-S International Microwave Symposium (IMS)*, 2017, pp. 529–532.

[7] A. P. Gregory and R. N. Clarke, "A review of RF and microwave techniques for dielectric measurements on polar liquids," *IEEE Trans. Dielectr. Electr. Insul.*, vol. 13, no. 4, pp. 727–743, Aug. 2006.

[8] D. J. Rowe, A. Porch, D. A. Barrow, and C. J. Allender, "Novel Coupling Structure for the Resonant Coaxial Probe," *IEEE Trans. Microw. Theory Tech.*, vol. 60, no. 6, pp. 1699–1708, Jun. 2012.

[9] A. Naylon, "Microwave resonant sensors," PhD, Cardiff University, 2011.

[10] R. A. Waldron, "Perturbation theory of resonant cavities," *Proc. IEE - Part C Monogr.*, vol. 107, no. 12, pp. 272–274, Sep. 1960.

[11] D. J. Rowe, A. Porch, D. A. Barrow, and C. J. Allender, "Microfluidic device for compositional analysis of solvent systems at microwave frequencies," *Sens. Actuators B Chem.*, vol. 169, no. Supplement C, pp. 213–221, Jul. 2012.

[12] S. Roy, "Microwave resonant sensor for measurement of ionic concentration in aqueous solutions," M.S. thesis, Electr. & Comptr. Engng., Iowa State Univ., Ames, IA, 2017.

[13] D. J. Rowe, "Microfluidic microwave resonant sensors," Ph.D. dissertation, School of Engng., Cardiff Univ., Cardiff, United Kingdom, 2012.

[14] R. N. Clarke, et al, "A guide to the characterisation of dielectric materials at RF and microwave frequencies," Institute of Measurement and Control/National Physical Laboratory, 2003.